J Electr Eng Technol.2017; 12(5): 1945-1954
http://doi.org/10.5370/JEET.2017.12.5.1945

ISSN(Print) 1975-0102
ISSN(Online) 2093-7423

LCL Filter Design Method for Grid-Connected PWM-VSC

Goran Majic†, Marin Despalatovic* and Bozo Terzic*

Abstract – In recent years, several LCL filter design methods for different converter topologies have been published, many of which use analytical expressions to calculate the ideal converter AC voltage harmonic spectrum. This paper presents the LCL filter design methodology but the focus is on presentation and validation of the non-iterative filter design method for a grid-connected three-phase two-level PWM-VSC. The developed method can be adapted for different converter topologies and PWM algorithms. Furthermore, as a starting point for the design procedure, only the range of PWM carrier frequencies is required instead of an exact value. System nonlinearities, usually omitted from analysis have a significant influence on VSC AC voltage harmonic spectrum. In order to achieve better accuracy of the proposed procedure, the system nonlinear model is incorporated into the method. Optimal filter parameters are determined using the novel cost function based on higher frequency losses of the filter. An example of LCL filter design for a 40 kVA grid-connected PWM-VSC has been presented. Obtained results have been used to construct the corresponding laboratory setup and measurements have been performed to verify the proposed method.

Keywords: Cost function, Grid-connected voltage source converters, Harmonic analysis, LCL filter, Non-iterative method, Optimization, Space vector pulse width modulation

1. Introduction

In order to connect adjustable speed drives or distributed power generation systems to the grid, three-phase pulse width modulation voltage source converters (PWM-VSC) are often used due to their controllability and higher efficiency compared to other converters [1]. Both two-level (2L) and three-level (3L) PWM-VSC topologies provide control of DC side voltage and power factor at the point of common coupling (PCC). Since implementation of PWM leads to occurrence of baseband and sideband harmonics in the AC voltage harmonic spectrum, a filter is needed to attenuate the grid current harmonics [2, 3]. Moreover, certain low-frequency current harmonics are influenced by system nonlinearities as well as the grid voltage harmonic distortion [4, 5]. The grid current harmonic limits defined by standards are stringent and much attention should be given to filter design [6, 7].

In most applications, L or LCL filters are used to comply with standards concerning the grid current harmonic limits [8]. Usage of LCL filters for grid connection of PWM-VSCs was first proposed in [9] because LCL filters provide higher attenuation of harmonics when compared to L filters with identical overall inductance. LCL filter main drawback is the resonance effect, but it can be alleviated using different passive and/or active damping methods. Regardless whether a damping method is used, the system performance in dynamic states and the overall system stability are directly influenced by the LCL filter parameters [10].

LCL filter design is a complex procedure involving various constraints, such as the grid current harmonic limits, the voltage drop across the filter inductors, the reactive power absorbed by the filter capacitors at fundamental frequency and the converter current ripple. Perhaps, the most important criterion for selection of LCL filter parameters is that the resonant frequency of the filter should not coincide with frequencies of switching harmonics to prevent excitation of the filter resonance effect. Although several papers concerning design of LCL filters for grid-connected PWM-VSCs have been published in the last decade, most methods have different drawbacks, one of which is their iterative character [11-28]. The design procedure reported in [11] was the first effective method for selection of filter parameters. Parameters are obtained from expressions involving the AC current ripple, the voltage drop across the filter inductors and the reactive power of the filter capacitors. Main drawbacks of this method are its iterative approach and the fact that most values of abovementioned expressions are not defined by standards concerning the allowed harmonic distortion of current at PCC [6, 7]. On the other hand, analytical expressions for the voltage harmonic spectrum of an ideal VSC together with the simplified LCL filter model are used to calculate the grid current harmonic spectrum in [12-15]. This allows for the comparison of current harmonic spectrum with limits defined by standards. The procedure in [16] combines previously published methods to clarify relationship among LCL filter parameters, the resonance

† Corresponding Author: Dept. of Power Engineering, University of Split, FESB, Croatia. (gomajic@fesb.hr)
* Dept. of Power Engineering, University of Split, FESB, Croatia. ({despi, bterzic}@fesb.hr)
Received: January 28, 2017; Accepted: June 4, 2017

frequency and the high frequency ripple attenuation. It is important to note that the presented approaches are characterized by the overall system simplifications that do not include system nonlinearities and grid voltage distortion. These simplifications, although practical, can lead to selection of inadequate LCL filter in terms of increased current harmonic distortion at PCC.

Logical extensions of methods for selecting LCL filter parameters are the filter optimization methods presented in [20-23]. These methods, although exhibiting common features, are developed for different converter topologies and modulation techniques. The Virtual Voltage Harmonic Spectrum (VVHS) concept developed in [24] is used as an integral part of the methods presented in [20, 21]. This concept assumes an ideal converter. Based on VVHS and an ideal filter model, worst-case grid current harmonic spectrum can be calculated and compared to standards [6, 7]. In order to decide the optimal combination of filter parameters from a set of parameter combinations which ensure that grid current harmonic content is within limits defined by standards, optimization methods use different criteria.

2. System Description

The three-phase 2L PWM-VSC connected to the grid through LCL filter, investigated in this paper, is shown in Fig. 1.

The grid is modelled with an ideal three-phase sinusoidal voltage source (v_{ag}, v_{bg}, v_{cg}) with fundamental frequency (f_n). Parameters L_{fg} and L_{fc} represent the grid side and the converter side inductor, respectively, while the parameter C_{fd} represents the filter capacitor. The nonlinear model of the presented system has been developed in PLECS and it includes the dead time delay [4, 29]. The system parameters are given in Table 1.

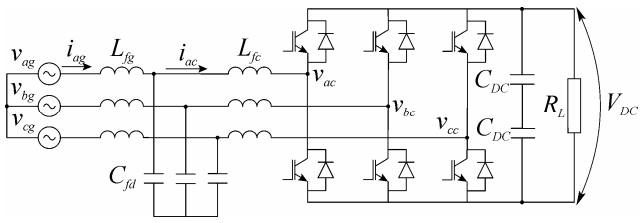

Fig. 1. Three-phase PWM-VSC connected to the grid through LCL filter

Table 1. Parameters of system shown in Fig. 1

Symbol	Quantity	Value
f_n	rated grid frequency	50 Hz
U_n	rated grid voltage (line-to-line, rms)	400 V
I_n	rated filter current (rms)	60 A
C_{DC}	DC link capacitance	3000 µF
V_{DC}	DC link voltage	620 V
f_c	carrier frequency	2 -5 kHz

3. LCL Filter Design Constraints and Optimization

Main goal of any filter design method is to select the filter that will provide sufficient attenuation of current harmonics at PCC. Considering the system parameters given in Table 1, two relevant standards that define the current harmonic limits at PCC when connecting electrical equipment to the grid are IEEE 519-2014 and IEC 61000-3-12 [6, 7]. In most cases, the first step of the filter design procedure is to define minimum and maximum values of filter parameters using different constraints and afterwards various optimization methods can be used to achieve lower filter losses and/or cost depending on selected criteria. In most cases, selection of filter parameters is a process that requires a certain number of iterations.

3.1 Filter parameters constraints

Typically, constraints used in filter design methods include the filter resonant frequency, the converter AC current ripple, the voltage drop across the filter inductors and the reactive power of the filter capacitors. These quantities are not defined by standards and their values differ among methods.

The converter AC voltage and the grid current harmonic spectra are mainly determined by the modulation technique and the synchronization between sampling and PWM algorithm execution implemented in the microcontroller as well as LCL filter parameters. The filter resonant frequency (f_{res}) should be chosen in such a manner to avoid excitation of resonance and to ensure stable operation of the overall system. This can be achieved if the following condition is met [2]

$$\left(10 \cdot f_n \text{ or } 0.25 \cdot f_c\right) < f_{res} < 0.5 \cdot f_c \qquad (1)$$

where the resonant frequency of the LCL filter is given by

$$f_{res} = \frac{1}{2\pi}\sqrt{\frac{L_{fg} + L_{fc}}{L_{fg} \cdot L_{fc} \cdot C_{fd}}} \qquad (2)$$

When calculating the resonant frequency, the grid impedance at PCC (and the impedance of isolating transformer) should be considered by increasing the grid side inductance.

The voltage drop across the filter inductors should not limit converter operation in the PWM linear region. The combined filter inductance is determined according to voltage drop at rated load and is usually chosen between 5 and 20% of the rated line-to-neutral grid voltage (V_n), [11]

$$0.05 \cdot V_n \le 2\pi \cdot f_n \cdot \left(L_{fc} + L_{fg}\right) \cdot I_n \le 0.2 \cdot V_n \quad (3)$$

where I_n is the filter (and/or PWM-VSC) rated AC current.

The converter AC current ripple is mainly limited by the converter side inductor. The minimum inductance value of the converter side inductor is determined by the maximum value of the converter AC current ripple ($\Delta I_{c,max}$) and can be chosen according to [13, 20]

$$L_{fc,\min} = \frac{V_{DC}}{k \cdot f_c \cdot \Delta I_{c,\max}} \quad (4)$$

where the coefficient k depends on the selected modulation technique.

When considering the filter capacitors, reactive power at f_n should be limited. If that is the case, the maximum value of capacitance is given by [17, 18]

$$C_{fd,\max} = \frac{\lambda \cdot P_n}{2\pi \cdot f_n \cdot (\sqrt{3} \cdot U_n)^2} \quad (5)$$

where P_n is the converter rated power and the coefficient λ depends on the maximum reactive power. The value of the coefficient λ is usually chosen between 0.05 and 0.1.

3.2 Filter parameters optimization methods

Filter optimization methods are often performed as a part of the filter design procedure to obtain the optimal combination of filter parameters from a set of allowed parameter combinations. This involves formulation of a criterion, i.e. a cost function (CF) used to select the optimal combination. As a starting point of the design procedure, most methods use various constraints, some of them given in previous section. Using these constraints, minimum and/or maximum values of filter parameters are calculated. For all parameter combinations, based on analytical expressions for the AC voltage harmonic spectrum of an ideal converter, the current harmonic spectrum at PCC is obtained and compared to the standards [6, 7]. This can be done for a single operating point or, as in case of VVHS concept, over entire range of operating points. Despite numerous differences between various filter design methods, they are all characterized by neglection of system nonlinearities and their influence on the AC voltage harmonic spectrum of PWM-VSC [20-22]. Because of this, selected filter parameters can lead to increased current harmonic distortion at PCC.

4. LCL Filter Design Method

4.1 Cost function

In most cases CFs are selected with a tendency to achieve low losses and/or low volume, i.e. price. Although it is possible to define various CFs and to select optimal parameter combinations accordingly, CFs which are compatible with the overall system design should be preferred. Selection of a certain optimal filter parameter combination can potentially lead to increased converter losses if the filter design is considered separately from the overall system design [22]. If the filter volume/mass is minimized, initial investment costs will be lower. However, it is the authors' opinion that the minimization of system losses will be more beneficial when considering long-term exploitation costs [30].

The main objective of this paper is to introduce the novel CF that will lead to reduction of both filter and converter losses. The converter switching and conduction losses mostly depend on the switching frequency, the DC link voltage, the pulse-width modulation index, the converter current and its spectrum, and semiconductors specifications [31]. On the other hand, inductor winding and core losses depend on current and flux density spectra [21, 32-34]. Hence, significant losses of the overall system can occur on higher frequencies. This suggests that overall system losses can be separated into two terms. The first term represents the fundamental component while the second term represents all other frequency components. The same approach, regarding voltage and current spectra, can be applied to the energy stored within filter components. Based on measurements performed as a part of this study, a correlation between higher frequency components of stored energy (reactive power) and losses can be established which is also valid for fundamental harmonic components. These observations indicate that the stored energy within filter components may be used to formulate CF while avoiding comprehensive winding and core losses modeling of filter inductors since they depend on numerous variables [33, 34]. Nevertheless, calculation of stored energy requires accurate determination of voltage and currents spectra which is achieved using the nonlinear model of the observed system [4]. By considering sources of system nonlinearities, error margin for the filter design procedure can be significantly decreased.

In this paper, CF includes reactive power within all filter components unlike in [20] where capacitors are neglected. Consequently, CF is defined as the inverse ratio between the fundamental reactive power of filter components and the sum of all other reactive power harmonic components

$$CF = \frac{\sum_{h=2}^{400} \omega_h \left(L_{fg} \cdot I_{gh}^2 + L_{fc} \cdot I_{ch}^2 + C_{fd} \cdot U_{fdh}^2\right)}{\omega_1 \left(L_{fg} \cdot I_{g1}^2 + L_{fc} \cdot I_{c1}^2 + C_{fd} \cdot U_{fd1}^2\right)} \quad (6)$$

where ω_1 and ω_h are the fundamental and the h-th harmonic angular frequency, I_{g1} and I_{c1} are the fundamental harmonics of the grid and the converter currents, I_{gh} and I_{ch} are the h-th harmonics of the grid and the converter

currents, U_{fd1} and U_{fdh} are the fundamental harmonic and the h-th harmonics of the filter capacitors voltages, respectively.

Numerator in (6) depends mainly on the harmonic distortion of grid and converter currents as well as the filter capacitors voltage. On the other hand, denominator represents only the fundamental harmonic and is a good indicator of the filter volume/price [35, 36]. It may be argued that the lower values of (6) will be achieved for those parameter combinations that ensure a relatively low harmonic distortion of converter and grid currents. If, for instance, L_{fg} is kept constant, this is accomplished with higher values of L_{fc} and lower values of C_{fd} in such a way to ensure that f_{res} complies with (1). Higher values of L_{fc} lead to lower converter current ripple which consequently results in lower converter and filter losses [34]. On the contrary, lower values of L_{fc} and higher values of C_{fd} may result in higher converter and filter losses. This is due to an increase in the fundamental reactive power of the capacitors, which requires a higher modulation index to achieve unity power factor at PCC [31].

4.2 Design procedure

The flowchart of the proposed LCL filter design method is presented in Fig 2. The first step of the design procedure is to define constraints based on initial input data. Converter topology and nominal data, modulation technique and carrier frequency as well as DC link voltage are used as a starting point for the procedure. Based on these data, minimum and/or maximum values of filter parameters and resonant frequency can be calculated according to (1) - (5). The next step is to choose resolution within previously defined ranges for every filter parameter. Although, at this point inductors resistances are not known since they depend on the dimensions and materials used for manufacturing, the equivalent series resistance (ESR) of a capacitor can be approximated according to available manufacturers' data. The ESR contributes to passive damping of the filter resonance.

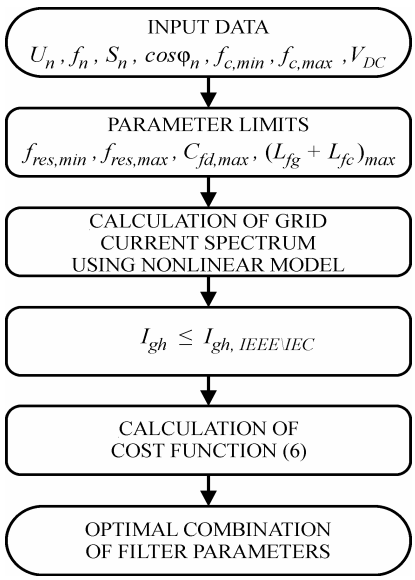

Fig. 2. Flowchart of proposed LCL filter design method

In the next step, the nonlinear model of the system is used to calculate the current harmonic spectrum at PCC for every parameter (L_{fg}, C_{fd}, L_{fc}) combination [4]. Furthermore, capacitors ESRs are incorporated into the model and it may be argued that those combinations that do not require additional passive damping are preferred. Simulation can be carried out for different operating points, but usually rated load for various power factors is chosen. By doing so, both standards given in Section 3 can be used in the design method since in [7] harmonic limits are defined in relation to the referent current. It should be pointed out that the inclusion of VVHS concept into design method would not allow for the use of [7] or implementation of the dead time nonlinearity since VVHS is obtained based on an ideal converter model.

The next step of the procedure is to determine the set of acceptable parameter combinations. This is achieved by comparing the grid current harmonics to limits defined by standards for every parameter combination. Cost function is calculated according to (6) for every combination of the obtained set. The main advantage of the presented design method is that the filter parameters are obtained in a straightforward way.

5. LCL Filter Design Example

In this section the proposed design method is used to select LCL filter parameters of a grid-connected three-phase 2L PWM-VSC. Parameters of the system are given in Table 1. Typically, the carrier frequency of a PWM-VSC can be varied over a defined range. In high power converters, maximum carrier frequency is limited to avoid excessive switching losses. The carrier frequency range in Table 1 is selected according to typical data of commercially available low-voltage converters when considering rated power up to 400 kVA. Double-edge symmetrical regularly sampled space vector pulse-width modulation (SVPWM) technique is implemented in the nonlinear model [3].

Aforementioned data and expressions (1), (3) and (5) are used to calculate the parameter limits. According to converter data and (1), the minimum value of f_{res} is set at 500 Hz while the maximum value depends on the carrier frequency. Based on (5), λ is set to 0.0786 in order to match the value of $C_{fd,max}$ to the standardized value of 65 μF [35]. The minimum capacitance value is chosen according to available catalogue data and is set at 10 μF [35]. The maximum allowed voltage drop across the filter inductors is 20% of the rated voltage, which corresponds to the maximum value of (L_{fg} + L_{fc}) equal to 2.46 mH. The

minimum inductance value for both filter inductors is set at 0.3 mH according to (3) which is sufficient to neglect the influence of the 1 MVA isolating transformer equivalent inductance (approx. 0.033 mH). Resolution for inductances is chosen to be 10 μH, while capacitances are chosen based on standard values for capacitors according to their type and intended purpose [35].

The filter design procedure can be carried out for different operating points considering both rectifier and inverter mode of operation as well as various (leading and lagging) displacement power factors. The range of considered operating points is limited by the condition of converter operation in the PWM linear region [1]. The design procedure is carried out for various operating points. However, only results for the rated operating point are presented for the sake of brevity because other operating points yielded similar results.

Since the exact value of the carrier frequency is not known prior to filter selection, the design procedure is carried out for carrier frequencies of 2, 3, 4 and 5 kHz. Based on the chosen resolution, the initial overall number of parameter combinations is 799695. For every parameter combination, the grid current harmonic spectrum is calculated using the nonlinear model of the system and combinations that do not comply with the standards are discarded. After this step, 189504 parameter combinations remain. Based on (6), the cost function is calculated for the remaining parameter combinations and the one with the minimum value can be selected as the optimal parameter combination.

Optimal parameter combinations for different f_c at $0.9I_n$ and unity power factor at PCC are given in Table 2. For all selected carrier frequencies, ratio f_c / f_n is an even number and the harmonic order (h) of fundamental frequency multiples around the first multiple of f_c are also even numbers. Because of this, all sideband harmonics for which $h \leq 50$ will be compared to more stringent limits since even harmonics are limited to 25% of odd harmonic limits [3, 6]. In accordance with abovementioned, none of the parameter combinations comply with the grid current harmonic limits for f_c = 2 kHz. Instead of 2 kHz, the procedure is repeated for f_c = 2.05 kHz.

Simulation results of grid current harmonic spectra, at $0.9I_n$ and unity power factor at PCC for parameter combinations given in Table 2, are presented in Fig. 3.

Table 2. Optimal Filter Parameter Combinations at $0.9I_n$ and Unity Power Factor

Carrier frequency (kHz)	Filter parameters				CF
	L_{fg} (mH)	L_{fc} (mH)	C_{fd} (μF)	f_{res} (Hz)	(VAr / VAr)
2.05	0.66	1.79	63	968	523 / 3315
3	0.72	1.73	63	893	328 / 3329
4	0.34	2.1	63	1172	190 / 3306
5	0.34	2.1	63	1172	146 / 3292

Presented harmonic spectra are obtained using the nonlinear model with dead time delay equal to 4 μs. Grid current harmonic limits defined by [6] for odd and even h are represented with blue and green solid lines, respectively, while dashed lines represent limits defined by older revision of the same standard for h > 50. Furthermore, only harmonics in the baseband and the first sideband region are presented since other harmonics in the grid current harmonic spectrum are negligible. Although, sideband harmonics are solely dependent on the PWM

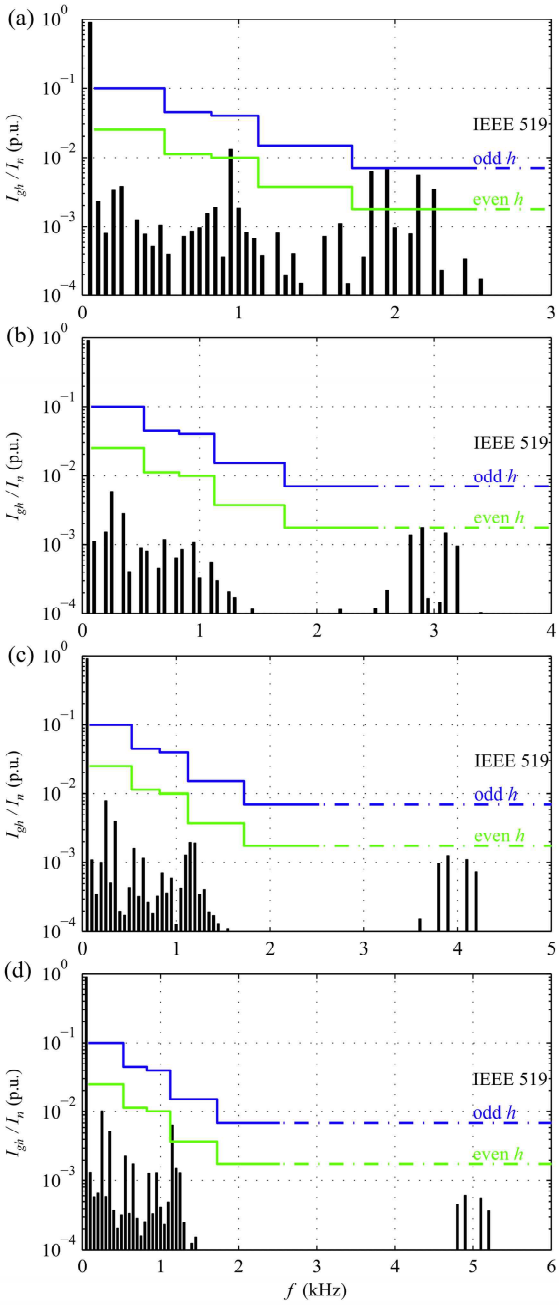

Fig. 3. Simulated grid current harmonic spectra at $0.9I_n$ and unity power factor at PCC for filter parameter combinations given in Table 2 and corresponding f_c: (a) 2.05 kHz, (b) 3 kHz, (c) 4 kHz, (d) 5 kHz

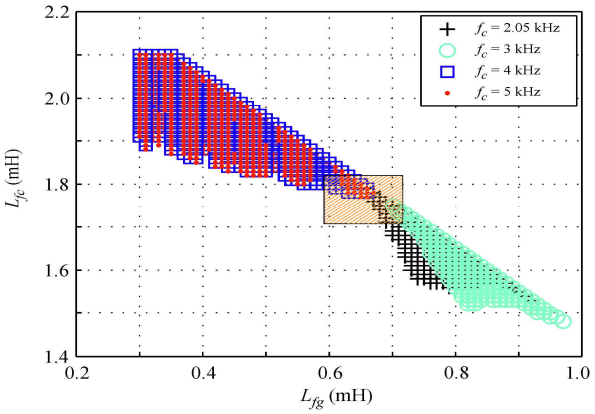

Fig. 4. Filter parameter combinations complying with $CF_{min} \leq CF \leq 1.2\ CF_{min}$

algorithm, some baseband harmonics are also influenced by the system nonlinearities as well as the LCL filter resonance effect [4].

In accordance with Table 2, the optimal filter capacitance is equal to 63 μF for all f_c but optimal values of inductances differ for both inductors. Clearly, there is no parameter combination that can be characterized as the optimal if f_c is not kept constant. Instead, it is necessary to determine a parameter combination that can be regarded as the most appropriate one, i.e. a compromise. In order to do so, four sets of parameter combinations are constructed for each of the four values of f_c given in Table 2 (2.05, 3, 4 and 5 kHz) and C_{fd} = 63 μF. Each set is constructed from parameter combinations for which the value of CF falls within the range defined by the minimum value of the cost function (CF_{min}) for a given f_c and a non-integer multiple (σ) of CF_{min}, i.e. $\sigma \cdot CF_{min}$. The value of parameter σ is varied until four sets of parameter combinations intersect, which occurs for σ = 1.2. If C_{fd} is kept constant, then four sets of parameter combinations can be presented as in Fig 4.

Combinations of each set are presented with an identical marker in the $L_{fg} - L_{fc}$ plane. Intersection between sets of markers occurs in the shaded area. Parameter combinations within the shaded area can be considered as a compromise if f_c is varied during exploitation. The boundaries of the shaded area in Fig. 4 are determined by taking into account tolerances of LCL filter components as defined in manufacturers' catalogues. It is reasonable to conclude that any parameter combination within the shaded area can be used to construct the LCL filter and final selection can be made based on availability of passive components.

6. Experimental Setup and Measurements

6.1 Laboratory setup

In order to validate the proposed LCL filter design method, laboratory setup was used for which the parameters are given in Tables 1 and 3. Laboratory setup, shown in Fig. 5, consists of a three-phase back-to-back converter connected to the grid through LCL filter. The grid side of the back-to-back converter is in accordance with Fig. 1 and is controlled using the voltage oriented control (VOC) method implemented in Texas Instruments' TMS320 F28335 microcontroller [1, 2]. The motor side of the converter is disconnected and an adjustable 35 kW resistive load is connected to the DC link bus.

Table 3. Parameters of Laboratory Setup

Symbol	Quantity	Value
L_{fg}	inductance of grid side filter inductors	0.6 mH
R_{fg}	resistance of grid side filter inductors	8 mΩ
L_{fc}	inductance of converter side inductors	1.8 mH
R_{fc}	resistance of converter side inductors	16 mΩ
C_{fd}	filter capacitance	60 μF
R_{fd}	capacitor equivalent series resistance	10 mΩ

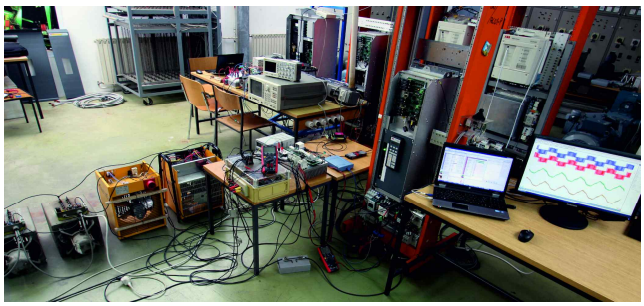

Fig. 5. Laboratory setup of system shown in Fig. 1

Due to limited availability of required passive elements and their individual price, the LCL filter is assembled using components listed in Table 3 [35, 36]. Selected inductors of the LCL filter fall within the shaded area in Fig 4.

Grid and converter voltages and currents are measured using voltage differential and current probes while the Hewlett Packard's digital signal analyzer HP35665A is used for online analysis of harmonic spectra.

6.2 Experimental Results

The purpose of experiments carried out on the laboratory setup is to verify the LCL filter effectiveness by measuring its losses and current harmonic spectrum at PCC for various operating points. Measurements of filter inductors losses and stored energy have been performed separately for each inductor and are used to illustrate the validity of the proposed CF [33, 34]. For the sake of clarity, only the losses of the converter side inductors for unity power factor at PCC are presented. Inductors total (P_{tot}) and fundamental harmonic (P_1) losses in relation to the converter current fundamental harmonic are shown in Fig. 6(a).

As can be seen, significant higher harmonic losses are present regardless of f_c. The rms value of the converter current without the fundamental harmonic is shown in Fig.

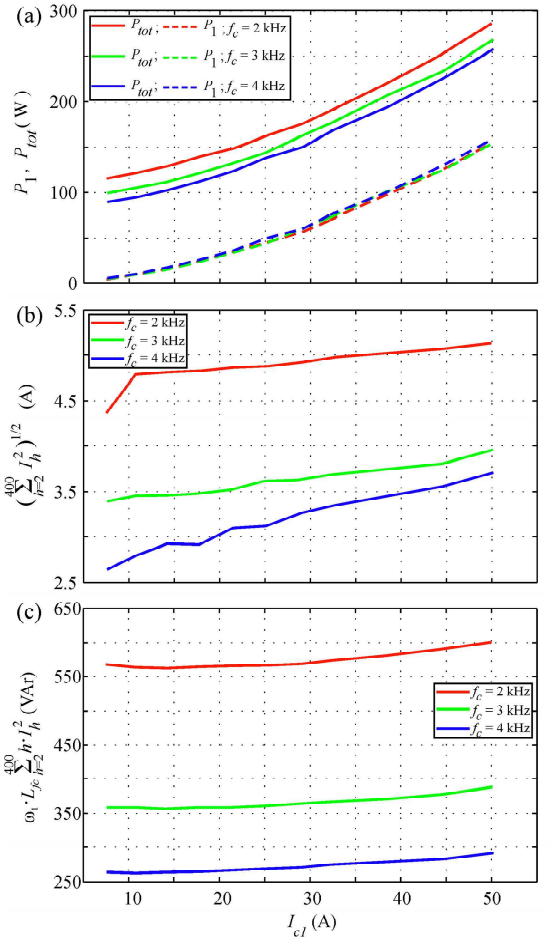

Fig. 6. Measurements on converter side inductors: (a) fundamental harmonic and total losses, (b) rms value of current without fundamental harmonic, (c) reactive power

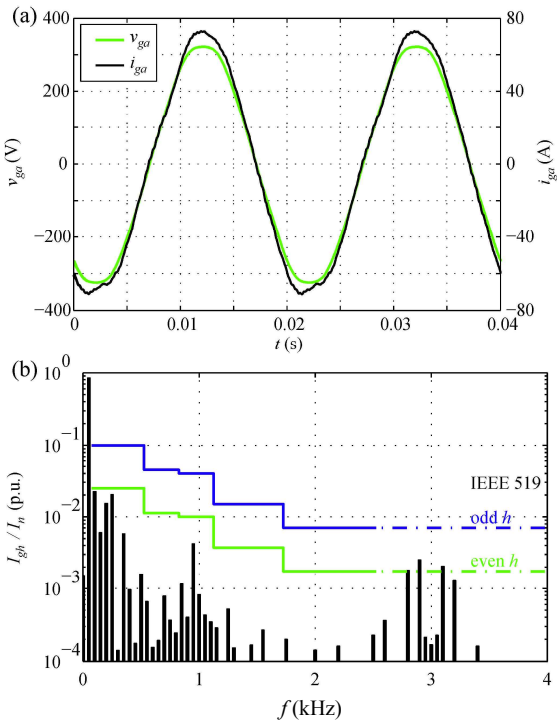

Fig. 7. Experimental results at 35 kW load and unity power factor at PCC for f_c = 3 kHz: (a) grid phase voltage and current waveforms, (b) grid current harmonic spectrum

6(b). This quantity varies with f_c and directly influences inductors total losses, i.e. stored energy shown in Fig. 6(c). Evidently, characteristics in Fig. 6 exhibit similar trends which justify the use of (6) as the CF for the LCL filter design method.

Measurements of current and voltage spectra on the AC side of PWM-VSC have been carried out for various operating points defined by different loads and power factors at PCC. The maximum load connected to the DC link bus is equal to 35 kW ($0.9I_n$ at unity power factor at PCC). For the sake of brevity, only results for this operating point and two different carrier frequencies are presented.

In Figs. 7 and 8, the grid phase voltage and current waveforms as well as the grid current harmonic spectra are shown for f_c of 3 and 4 kHz, respectively. As can be seen from Figs. 7a and 8a, grid voltages and currents are in phase and both waveforms exhibit non-ideal sine waveform. The grid current waveform suggests that certain low-order even harmonics are present in the spectrum. This is observed for all operating points and confirmed by the corresponding grid current spectra for carrier frequencies of 3 and 4 kHz, shown in Figs. 7(b) and 8(b), respectively. The grid current harmonic limits defined by [6] are represented with the blue (odd h) and the green (even h) solid line with dashed lines corresponding to limits given by older revision of the same standard for $h > 50$. Low-order harmonics occur throughout the baseband region as a consequence of the PWM algorithm. When calculated according to analytical expressions for an ideal converter, magnitudes of these harmonics are lower by as much as an order of magnitude [3]. One possible explanation for discrepancies concerning these harmonics is that their magnitudes are largely determined by unavoidable presence of nonlinearities in the laboratory setup [4]. Additionally, current harmonics around 1 kHz are influenced by the filter resonance effect since the LCL filter resonance frequency is 968 Hz. Also, the grid voltage distortion impacts the grid current spectrum in the baseband region.

The grid current harmonic spectrum shown in Fig. 7(b) complies with harmonic limits defined by [6]. Since harmonic orders of the first sideband harmonics are even numbers this would not be the case if they are compared to the older revision of the same standard. This is consistent with simulation results presented in Section 5. For f_c = 4 kHz, the LCL filter provides sufficient attenuation of sideband harmonics as shown in Fig. 8(b).

Based on the analysis of experimental results, the choice

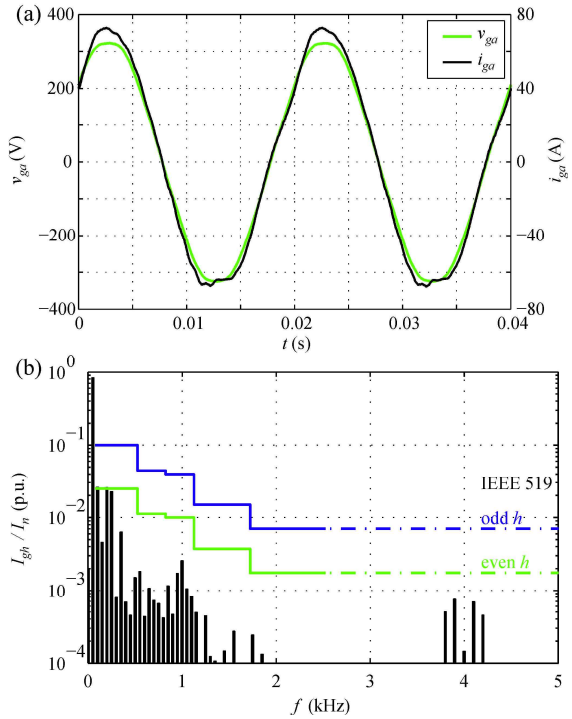

Fig. 8. Experimental results at 35 kW load and unity power factor at PCC for f_c = 4 kHz: (a) grid phase voltage and current waveforms, (b) grid current harmonic spectrum

of f_c is very important since harmonic limits imposed by standards are very stringent, especially for f_c < 2.5 kHz. However, the proposed LCL filter design method does not require knowing the exact value of f_c. After the LCL filter has been constructed in accordance with the results of the filter design method, it is possible to select the optimal f_c based on certain criteria.

7. Conclusions

In this paper, the non-iterative LCL filter design method is based on the novel cost function. Proposed CF, although formulated in accordance with measurements of inductors losses, requires calculation of reactive power within filter components instead of losses. Exact calculation of losses requires numerous data concerning geometry and materials used for filter construction. On the other hand, calculation of reactive power is based on the nonlinear model since analytical expressions of the ideal converter AC voltage spectrum exhibit significant differences in comparison to measured results. In other words, implementation of the nonlinear model increases accuracy of the proposed method. The described approach is focused on increasing overall system efficiency during design stage instead of minimizing filter volume/price. This concept is chosen because it is compatible with further online optimization of the system during the exploitation stage, e.g. by selecting the optimal carrier frequency, which will be the subject of future work.

Acknowledgements

This work has been supported by Croatian Science Foundation under the project Metrological infrastructure for smart grid IP-2014-09-8826.

References

[1] M. Kazmierkowski, R. Krishnan, F. Blaabjerg, *Control in Power Electronics, Selected Problems*, Academic Press, Oxford, 2002.

[2] J. Dannehl, C. Wessels, F.W. Fuchs, "Limitations of Voltage-Oriented PI Current Control of Grid-Connected PWM Rectifiers With LCL Filters", *IEEE Trans. Ind. Electron.*, vol. 56, no. 2, pp. 380-388, Feb. 2009.

[3] D. G. Holmes, T. A. Lipo, *Pulse Width Modulation for Power Converters, Principles and Practice*, IEEE Press, Piscataway, NJ, 2003.

[4] G. Majic, M. Despalatovic, K. Verunica, "Influence of Dead Time on Voltage Harmonic Spectrum of Grid-Connected PWM-VSC with LCL Filter", *in Proc. of Int. Conf. on Compatibility, Power Electronics and Power Engineering (CPE-POWERENG)*, pp. 228-233, Bydgoszcz, June/July 2016.

[5] R. J. Kerkman, D. Leggate, D. W. Schlegel, C. Winterhalter, "Effects of Parasitics on the Control of Voltage Source Converters", *IEEE Trans. Power Electron.*, vol. 18, no. 1, pp. 140-150, March, 2003.

[6] Institute of Electrical and Electronics Engineers, *IEEE Recommended Practices and Requirements for Harmonic Control in Electrical Power Systems - IEEE Std 519-2014 (Revision of IEEE Std 519-1992)*, New York, 2014.

[7] International Electrotechnical Commission, *Electro-magnetic Compatibility (EMC) Part 3-12: Limits for harmonic currents produced by equipment connected to public low-voltage systems with input current >16 A and ≤75 A per phase – IEC 61000-3-12 (Edition 2.0 2011-05)*, Geneva, 2011.

[8] R. Beres, X. Wang, F. Blaabjerg, C.C. Bak, M. Liserre, "A Review of Passive Filters for Grid-Connected Voltage Source Converters", *in Proc. of IEEE Applied Power Electronics Conf. and Expo. (APEC)*, pp. 2208–2215, Fort Worth (TX), March 2014.

[9] M. Lindgren, J. Svensson, "Connecting Fast Switching Voltage-Source Converters to the Grid – Harmonic Distortion and its Reduction", *in Proc. of IEEE Power Tech Conf.*, pp. 191-196, Stockholm, June 1995.

[10] J. Dannehl, F.W. Fuchs, S. Hansen, "PWM Rectifier with LCL-Filter using different Current Control Structures", *in Proc. of European Conf. on Power Electronics and Applications*(*EPE*), pp. 1-10, Aalborg, Sep. 2-5. 2007.

[11] M. Liserre, F. Blaabjerg, S. Hansen, "Design and control of an LCL-filter-based three-phase active rectifier", *IEEE Trans. Ind. Appl.*, vol. 41, no. 5, pp. 1281-1291, Sep./Oct. 2005.

[12] K.-J. Lee, N.-J. Park, R.-Y. Kim, D.-H. Ha, D.-S. Hyun, "Design of an LCL Filter employing a Symmetric Geometry and its Control in Grid-connected Inverter Applications", *in Proc. of the IEEE Power Electronics Specialists Conf. (PESC)*, pp. 963-966, Rhodes, June 2008.

[13] K. Jalili, S. Bernet, "Design of LCL Filters of Active-Front-End Two-Level Voltage-Source Converters", *IEEE Trans. Ind. Electron.*, vol. 56, no. 5, pp. 1674-1689, May 2009.

[14] B.-G. Cho, S.-K. Sul, "Non-iterative LCL Filter Design for Three-Phase Two-Level Voltage-Source Converters", *in Proc. of Int. Power Electronics Conf. (IPEC)*, pp. 2802-2809, Hiroshima, May 2014.

[15] G. Gohil, L. Bede, R. Teodorescu, T. Kerekes, F. Blaabjerg, "Line Filter Design of Parallel Interleaved VSCs for High-Power Wind Energy Conversion Systems", *IEEE Trans. Power Electron.*, vol. 30, no.12, pp. 6775-6790, Dec. 2015.

[16] F. Liu, X. Zha, Y. Zhou, S. Duan, "Design and Research on Parameter of LCL filter in Three-Phase Grid-Connected Inverter", *in Proc. of IEEE 6th Int. Power Electronics and Motion Control Conf.* (*IPEMC*), pp. 2174-2177, Wuhan, May 2009.

[17] B. Parikshith, V. John, "Filter Optimization for Grid Interactive Voltage Source Inverters", *IEEE Trans. Ind. Electron.*, vol. 57, no. 12, pp. 4106-4114, Dec. 2010.

[18] T. Wang, Z. Ye, G. Sinha, X. Yuan, "Output Filter Design for a Grid-interconnected Three-Phase Inverter", *in Proc. of IEEE Power Electronics Specialists Conf.* (*PESC*), vol.2, pp.779-784, Acapulco, June 2003.

[19] H. M. Ahn, C.-Y. Oh, W.-Y. Sung, J.-H. Ahn, B. K. Lee, "Analysis and Design of LCL Filter with Passive Damping Circuits for Three-phase Grid-connected Inverters", *Journal of Electrical Engineering and Technology*, vol. 12, no. 1, pp. 217-224, 2017.

[20] R. Meyer, A. Mertens, "Design of LCL Filters in Consideration of Parameter Variations for Grid-Connected Converters", *in Proc. of IEEE Energy Conversion Congress and Expo. (ECCE)*, pp. 557-564, Raleigh (NC), Sept. 15-20. 2012.

[21] J. San-Sebastian, I. Etxeberria-Otadui, A. Rujas. J. A. Barrena, P. Rodriguez, "Optimized LCL Filter Methodology Applied to MV grid-connected Multi-megawatt VSC", *in Proc. of IEEE Energy Conversion Congress and Expo. (ECCE)*, pp. 2506-2512, Raleigh (NC), Sept. 15-20. 2012.

[22] J. Mühlethaler, M. Schweizer, R. Blattmann, J. W. Kolar, A. Ecklebe, "Optimal Design of LCL Harmonic Filters for Three-Phase PFC Rectifiers", *IEEE Trans. Power Electron.*, vol. 28, no. 7, pp. 3114-3125, July 2013.

[23] H. Zheng, Z.-F. Liang, M.-S. Li, K. Li "Optimization of Parameters for LCL Filter of Least Square Method Based Three-phase PWM Converter", *Journal of Electrical Engineering and Technology*, vol. 10, no. 4, pp. 1626-1634, 2015.

[24] A. A. Rockhill, M. Liserre, R. Teodorecsu, P. Rodriguez, "Grid-Filter Design for a Multimegawatt Medium-Voltage Voltage-Source Inverter", *IEEE Trans. Ind. Electron.*, vol. 58, no. 4, pp. 1205-1217, April 2011.

[25] E. Kantar, A. M. Hava, "Design of Grid Connected PWM Converters Considering Topology and PWM Methods for Low-Voltage Renewable Energy Applications", in Proc. of Int. Power Electronics Conf. (IPEC), pp. 2034-2041, Hiroshima, May 2014.

[26] A. Reznik, M. G. Simões, A. Al-Durra, S. M. Muyeen, "LCL Filter Design and Performance Analysis for Grid-Interconnected Systems", *IEEE Trans. Ind. Appl.*, vol. 50, no. 2, pp. 1225-1232, Mar./Apr. 2014.

[27] R. Peña-Alzola, M. Liserre, F. Blaabjerg, M. Ordonez, Y. Yang, "LCL-Filter Design for Robust Active Damping in Grid-Connected Converters", *IEEE Trans. Ind. Informat.*, vol. 10, no. 4, pp. 2192-2203, Nov. 2014.

[28] Q. Liu, L. Peng, Y. Kang, S. Tang, D. Wu, Y. Qi, "A Novel Design and Optimization Method of an LCL Filter for a Shunt Active Power Filter", *IEEE Trans. Ind. Electron.*, vol. 61, no. 8, pp. 4000-4010, Aug. 2014.

[29] "PLECS User Manual (v3.7)", Plexim GmbH, Zurich, 2015. Available: http://www.plexim.com/ download/ documentation

[30] "Premium Efficiency Motor Selection and Application Guide, A Handbook for Industry", US Department of Energy, 2014. Available: https://www.energy.gov/sites/prod/files/2014/04/f15/amo_motors_handbook_web.pdf

[31] M. H. Bierhoff, F. W. Fuchs, "Semiconductor losses in Voltage Source and Current Source IGBT Converters Based on Analytical Derivation", *in Proc. of IEEE Annual Power Electronics Specialists Conf. (PESC)*, vol. 4, pp. 2836-2842, Aachen, June 20-25. 2004.

[32] A. V. den Bossche, V. C. Valchev, *Inductors and Transformers for Power Electronics*, CRC Press / Taylor Francis Group, Boca Raton, FL, 2005.

[33] J. Mühlethaler, J. Biela, J.W. Kolar, A. Ecklebe, "Improved Core-Loss Calculation for Magnetic Components Employed in Power Electronic Systems, *IEEE Trans. Power Electron.*, vol. 27, no. 2, pp. 964-

973, July 2012.
[34] J. Mühlethaler, J. W. Kolar, A. Ecklebe, "Loss Modeling of Inductive Components Employed in Power Electronic Systems", *in Proc. of IEEE Int. Conf. on Power Electronics and ECCE Asia* (*ICPE & ECCE*), pp. 945-952, Jeju, May/June 2011.
[35] "Film Capacitors – Power Electronic Capacitors, General purpose applications, ver. 5.0", EPCOS, TDK Group, 2013. Available: http://en.tdk.eu/inf/ 20/50/ds/ B3236_.pdf
[36] Reactors and ECOsine Passive Harmonic Filter, Schaffner Group, 2016. Available: http://www.schaffner.com/products/power-quality/ecosine-passive-harmonic-filter/all-products/

Goran Majić received the B.S. and Ph.D. degrees in electrical engineering from the Faculty of Electrical Engineering, Mechanical Engineering and Naval Architecture (FESB), University of Split, Split, Croatia, in 2006 and 2014, respectively. Since 2008 he has been in the Department of Electrical Power Engineering at FESB as a Research Assistant. His research interests include electrical machines and drives, in particular, grid-connected voltage source converters. He is currently a Postdoctoral Fellow at FESB.

Marin Despalatović received the B.S. and Ph.D. degrees in electrical engineering from the Faculty of Electrical Engineering, Mechanical Engineering and Naval Architecture, University of Split, Split, Croatia, in 2000 and 2009, respectively. Since 2001 he has been in the Department of Electrical Power Engineering at the University of Split as a Research Assistant. His research interests include electrical machines and drives, in particular, modeling and parameter identifycation of electric machines. He is currently an Associate Professor at FESB.

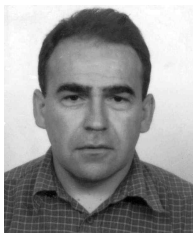

Bozo Terzić received the B.S. and Ph.D. degrees in electrical engineering from the Faculty of Electrical Engineering, Mechanical Engineering and Naval Architecture, University of Split, Split, Croatia, in 1986 and 1998, respectively, and the M.S. degree from the Faculty of Electrical Engineering, University of Zagreb, Croatia, in 1993. In 1986, he became an Assistant in the Department of Electrical Power Engineering, Faculty of Electrical Engineering, Mechanical Engineering and Naval Architecture, University of Split, where, since 2009, he has been a Full Professor. His research interests include ac electrical machines and drives.